Design and Prototyping of a Multi-Turn Sinusoidal Air-gap Length Resolver

H. Saneie, *Student Member, IEEE*, Z. Nasiri-Gheidari, *Senior Member, IEEE*, and F. Tootoonchian, *Senior Member, IEEE*

***Abstract*—Multi-turn resolvers are employed in the applications that high reliability; high accuracy and absolute position measurement are required, simultaneously. They are basically consisted of two individual resolvers in a common frame. In this paper a novel sinusoidal air-gap length multi-turn resolver is proposed. The rotor shape and the winding configuration are designed to achieve single-speed and multi-speed operations using a single rotor and a single stator core. Furthermore, some constraints are laid down and discussed in such a way that the performance of two resolvers has no interference with each other. All the mathematical calculations are validated using time stepping finite element analysis. Finally, a prototype of the sensor is built and tested. Experimental measurements are used to verify the analytical and finite element discussions.**

***Index Terms*— Multi-turn resolver, Multi-speed resolver, Variable reluctance (VR) resolver, Design, Time Stepping Finite Element Analysis (TSFEA).**

NOMENCLATURE

$a/\ a_k/\ b/\ \delta_k$	Different parameter related to the shape of rotor contour
$d\rho_i/\ \rho_i$	Permeance element/ permeance between one stator tooth and the rotor
i	Index of stator teeth number
k, j	Harmonic order
n, m	Arbitrary integer number
$g(\varphi,\theta_r)$	Air gap length
g_{max}	Maximum air gap length
$r_{shaft}/\ r_{si}$	Radius of rotor shaft/ stator bore
x_1	stator tooth width
L	Stack length of resolver
$N_{c.i}/\ N_{s.i}$	Number of Cosine/ Sine winding's coil turn around the ith tooth
N_{max}	Maximum Number of coil turn
P, P_k, P_j	Number of pole pairs
P_w	Signal windings' pole number
$V_{exc}/\ V_c$	The induced voltage in the Excitation/ cosine winding
V_i	the envelope of the induced voltage on one turn of the coil around the ith tooth
$V_{c0}/V_{ck}/\ V_{cj}$	dc component/ kth/ jth order harmonic of V_i
Z	Number of stator teeth
$\theta_r/\ x_r$	Rotor position in polar/ cartesian coordinate system
μ_0	Permeability of vacuum
φ	Angular coordinate

This work is supported in part by Niroo Research Institute (NRI), Sharif University of Technology, and Iran National Science Foundation (INSF).

H. Saneie and Z. Nasiri-Gheidari, are with Electrical Engineering Department, Sharif University of Technology, Tehran, Iran (Email: hamid.saneie@gmail.com, and znasiri@sharif.edu). F. Tootoonchian is with Electrical Engineering Department, Iran University of Science and Technology (IUST), Tehran, Iran, (Email: tootoonchian@iust.ac.ir).

I. INTRODUCTION

Multi-turn and multi-speed concepts are sometimes used instead. To explain the difference, it should be mentioned that "speed" refers to the number of pole pairs. It means a single speed sensor, so-called 1-X sensor, has one pole pair and a five speed one, 5-X sensor, has 10-pole. While, "turn" refers to the number of individual resolvers in one frame. Usually, a multi-turn resolver is consisted of two individual resolvers in one frame [1]. There are two types of multi-turn resolvers: gearless and geared ones. Gearless multi-turn resolvers that are briefly called multi-turn resolvers are consisted of two single-speed and multi-speed resolver. Using two resolvers not only improve the reliability of the multi-turn sensors, but also leads to provide the benefits of higher accuracy and absolute measurement, simultaneously [2]- [3]. On the other hand, geared resolver is also included two individual resolvers that are coupled to each other through a gear train. One of the resolvers, called fine resolver, is directly coupled to the machine shaft and rotates with the equal speed of the machine. While, the other resolver, called coarse resolver, is geared down by the used gear ratio [4]. The most common gear ratios are 1:8, 1:16, 1:32, and 1:36 but other ratios can be found, too [5].

Although single-speed and multi-speed resolvers have increasingly got researchers' attention in recent years, multi-turn resolvers are less involved in the literature. Most of the single-speed resolvers in literature have wound rotor (WR) or variable reluctance sinusoidal area (VR-SA) configurations. Optimal design [6]- [8], performance analysis [9]- [10], performance prediction under fault conditions [11]- [16] are the main subjects of the works on 2-pole resolvers. The preferred configurations of multi-speed resolvers are variable reluctance sinusoidal air-gap length (VR-SAGL) and WR with fractional slot winding. Geometrical optimizations [17]- [18], winding proposal [19]- [25], performance improvement [26]- [27] are the main research topics of multi-speed resolvers.

The literature referred to multi-turn resolvers are divided into two groups. The first group involves the researches that introduce different configurations of multi-turn resolvers or a short description of their different types, without any technical discussions [3]- [5], [28]- [31]. The next group is consisted of

deep scientific researches on optimal design, and performance evaluation of multi-turn resolvers [1]- [2]. In [1] a VR multi-turn resolver is designed and optimized to achieve higher accuracy, lower size, and higher stability under mechanical faults. The optimized resolver of [1] is consisted of a disk type 5-X sinusoidal air-gap length resolver and a 1-X disk type sinusoidal area one. The performance characteristics of the resolver are discussed and optimized under different mechanical faults and finally a prototype of the sensor is built and tested. In [2] a multi-turn WR resolver is proposed. Different slot-pole combinations and winding configurations are examined to be able to use identical cores for both 1-X and 5-X resolvers. In both multi-turn resolvers of [1]- [2] two stator cores and two rotor cores are employed and different optimizations are done to reduce the size and the cost of the sensors. In this paper design considerations of a novel multi-turn VR resolver with only one stator core and one rotor core for both 1-X and 5-X resolvers are discussed. The possibility of such design and its constraints are mathematically formulated. Afterwards, the presented analytical model is approved using 3-D time stepping finite element analysis. Finally, a prototype of the proposed resolver is built and tested. Experimental measurements verify the success of the proposed resolver.

II. Proposed Multi-turn Resolver

To describe the performance of the proposed multi-turn resolver it is required to review the operating principle of the conventional VR resolvers. A commercial VR resolver has a solid rotor whose air-gap length varies as [22]:

$$g(\varphi,\theta_r) = \frac{b}{1 + a\cos P(\varphi - \theta_r)} \tag{1}$$

where φ denotes the angular coordinate, θ_r rotor position, P rotor saliencies, b, and a length and shape factors, respectively. Considering the air-gap length as (1) causes sinusoidal variation of air-gap permeance that leads to pass a flux from the stator teeth. That flux in the ideal form has a DC component plus a sinusoidal component corresponds to the resolver pole number and a function of rotor position.

Furthermore, the relation between the stator teeth, Z, and rotor poles, P, can be presented as [25]:

$$P \pm P_w = \frac{KZ}{2} \tag{2}$$

where P_w is the signal windings' pole number, and K is an odd integer. Then, the signal windings' turn number, $N_{s,i}$ and $N_{c,i}$, can be calculated as [25]:

$$N_{s.i} = N_{max} \times sin\, P_w \left[\frac{2\pi}{Z}(i-1)\right] \tag{3}$$

$$N_{c.i} = N_{max} \times cos\, P_w \left[\frac{2\pi}{Z}(i-1)\right] \tag{4}$$

where N_{max} is the maximum number of coil turns, and i is the teeth number. The sinusoidal change of signal windings' turn number with P_w that is calculated by (2), leads to omit the DC component of the flux. Hence, the signal windings' flux linkage will be a sinusoidal function of the rotor position.

The main idea of the proposed multi-turn resolver originates from here that the rotor contour can be designed in such a way that the flux passing through the stator teeth has two or more desired sinusoidal components (pole numbers) instead of one. However, the main constraint is the stator windings must be designed in such a way that two speeds of resolver have no interference with each other.

Finally, the excitation winding is wound on all stator teeth with alternatively changed direction and a constant turn number. That configuration of excitation winding helps to omit the excitation flux harmonics and keeping its DC component. It means the self-inductance of the excitation winding will be constant.

To sum up if the air-gap length is designed to has desirable harmonics corresponds to desirable pole numbers, the required signal windings pole number can be determined from (2) and their turn number can be calculated using (3) -(4).

III. Mathematical Formulation

In this section the rotor contour is designed to have desirable harmonic components in the teeth flux. In this regards, the desirable harmonics are determined and their interference with the operating performance of the resolver is discussed.

Assuming the envelope of the induced voltage on the i[th] tooth as:

$$V_i = \left\{V_{c0} + \sum_{k=1}^{\infty} V_{ck} \sin\, P_k\left(\theta_r - \frac{2\pi}{Z}(i-1)\right)\right\} \times \cos\big(\pi(i-1)\big) \tag{5}$$

where P_k is an integer indicating the desirable pole number (harmonic order). Considering the turn number of the cosine winding as (4), the induced voltage in the cosine winding can be calculated as:

$$V_c = \sum_{\substack{i=1 \\ i\ is\ odd}}^{Z} V_{c0} \cos\left(\frac{P_w 2\pi}{Z}(i-1)\right) - \sum_{\substack{i=1 \\ i\ is\ even}}^{Z} V_{c0} \cos\left(\frac{P_w 2\pi}{Z}(i-1)\right) + \sum_{\substack{i=1 \\ i\ is\ odd}}^{Z} \sum_{k=1}^{\infty} V_{ck} \cos\left(\frac{P_w 2\pi}{Z}(i-1)\right) \times \sin\, P_k\left(\theta_r - \frac{2\pi}{Z}(i-1)\right) - \sum_{\substack{i=1 \\ i\ is\ even}}^{Z} \sum_{k=1}^{\infty} V_{ck} \cos\left(\frac{P_w 2\pi}{Z}(i-1)\right) \times \sin\, P_k\left(\theta_r - \frac{2\pi}{Z}(i-1)\right) \tag{6}$$

However, the constraints of determining the desirable harmonics, windings arrangement and the resolver's parameters should be determined in continue.

This article has been accepted for publication in a future issue of this journal, but has not been fully edited. Content may change prior to final publication. Citation information: DOI 10.1109/TEC.2019.2945120, IEEE Transactions on Energy Conversion

A. Influence of Harmonics on Self-Inductance of Excitation Inductance

As mentioned earlier, for the acceptable performance of the resolver the self-inductance of the excitation winding should be constant value. Hence, the constraint to keep it constant should be determined. In this regards, considering P_w=*Z/2*, the excitation voltage is calculated as:

$$V_{exc} = \sum_{i=1}^{Z} V_{c0} + \sum_{k=1}^{\infty} V_{ck} \sum_{i=1}^{Z} \sin\ P_k \left(\theta_r - \frac{2\pi}{Z}(i-1)\right) \tag{7}$$

The first term is V_{c0}Z, while the second term is calculated based on different values for $\frac{P_k}{Z}$ as:

$$\sum_{i=1}^{Z} \sin P_k \left(\theta_r - \frac{2\pi}{Z}(i-1)\right) = \begin{cases} Z \sin P_k\theta_r\ ; \frac{P_k}{Z} = n \\ 0 \qquad\quad ; \frac{P_k}{Z} = \frac{n}{m} \end{cases} \tag{8}$$

Where n, and m are integers and $\frac{n}{m}$ is not integer. Finally, it can be concluded if P_k is not integral multiple of Z, the envelope of excitation voltage will be constant ($\boldsymbol{V_{exc} = V_{c0}Z}$). Therefore, the self-inductance of the excitation inductance will be constant.

B. Influence of Harmonics on Mutual-Inductances

To ensure the signal windings magnify the harmonic referred to P pole number, (2) must be satisfied. For P=P_j, and K=1, let assume winding pole pairs as:

$$\left(P_j - \frac{Z}{2}\right) = P_w \tag{9}$$

Substituting (9) into (6) and doing some simplifications, leads to:

$$\begin{aligned} V_c = V_{c0} \sum_{i=1}^{Z} \cos\left(\frac{P_j}{Z} 2\pi(i-1)\right) \\ + \sum_{k=1}^{\infty} V_{ck} \sum_{i=1}^{Z} \cos P_j \left(\frac{2\pi}{Z}(i-1)\right) \\ \times \sin\ P_k \left(\theta_r - \frac{2\pi}{Z}(i-1)\right) \end{aligned} \tag{10}$$

Ideally the first term must be zero and only the main harmonic (the second term) must be existed in the output voltage. As described for excitation voltage, (8), to omit the first term P_j is not allowed to be an integral multiple of Z. Then, the second term considering P_k not to be an integral multiple of Z can be simplified as:

$$\begin{aligned} V_c = \frac{ZV_{cj}}{2} \sin\ P_j\theta_r \\ + \frac{V_{cj}}{2} \sum_{i=1}^{Z} \sin\ P_j \left(\theta_r - \frac{4\pi}{Z}(i-1)\right) \\ + \sum_{\substack{k=1 \\ k\neq j}}^{\infty} \frac{V_{ck}}{2} \sum_{i=1}^{Z} \left\{ \sin\ P_k \left(\theta_r + \left(\frac{P_j}{P_k} - 1\right)\frac{2\pi}{Z}(i-1)\right) \right. \\ \left. + \sin\ P_k \left(\theta_r - \left(\frac{P_j}{P_k} + 1\right)\frac{2\pi}{Z}(i-1)\right) \right\} \end{aligned} \tag{11}$$

To omit the second term of (11), $\frac{2P_j}{Z}$ must not to be an integral integer of *Z*. Finally, considering P_k, P_j, and $2P_j$ not to be integral integer of Z, the induced voltage can be written as:

$$\begin{aligned} V_c = \frac{ZV_{cj}}{2} \sin\ P_j\theta_r \\ + \sum_{\substack{k=1 \\ k\neq j}}^{\infty} \frac{V_{ck}}{2} \sum_{i=1}^{Z} \left\{ \sin\ P_k \left(\theta_r + \left(\frac{P_j}{P_k} - 1\right)\frac{2\pi}{Z}(i-1)\right) \right. \\ \left. + \sin\ P_k \left(\theta_r - \left(\frac{P_j}{P_k} + 1\right)\frac{2\pi}{Z}(i-1)\right) \right\} \end{aligned} \tag{12}$$

In single turn resolvers there is only one P_k for the sensor. Therefore, the induced voltage of (12) can be written for single turn resolvers as:

$$V_c = \frac{ZV_{cj}}{2} \sin\ P_j\theta_r \tag{13}$$

While for multi-turn resolvers it is supposed to have two or more values for P_k. Hence, it is required to find the constraints that must be considered to have no interference with different speeds operation. In this regards the second term of (12), considering $P_k \neq P_j$ is re-written as:

$$\begin{aligned} \sum_{i=1}^{Z} \sin\ P_k \left(\theta_r + \left(\frac{P_j}{P_k} - 1\right)\frac{2\pi}{Z}(i-1)\right) \\ + \sum_{i=1}^{Z} \sin\ P_k \left(\theta_r - \left(\frac{P_j}{P_k} + 1\right)\frac{2\pi}{Z}(i-1)\right) \end{aligned} \tag{14}$$

The first and the second terms of (14) are calculated as:

$$\begin{aligned} \sum_{i=1}^{Z} \sin\ P_k \left(\theta_r + \left(\frac{P_j}{P_k} - 1\right)\frac{2\pi}{Z}(i-1)\right) \\ = \begin{cases} Z \sin\ P_k\theta_r & \frac{P_j - P_k}{Z} = n \\ 0 & \frac{P_j - P_k}{Z} = \frac{n}{m} \end{cases} \end{aligned} \tag{15}$$

$$\sum_{i=1}^{Z} \sin\ P_k\left(\theta_r - \left(\frac{P_j}{P_k}+1\right)\frac{2\pi}{Z}(i-1)\right) = \begin{cases} Z\sin\ P_k\theta_r & \frac{P_j+P_k}{Z} = n \\ 0 & \frac{P_j+P_k}{Z} = \frac{n}{m} \end{cases} \quad (16)$$

where n, and m are integers and n/m is not integer.

Finally, the following conditions must be included to ensure the additional harmonics to the flux of teeth have no interference with each other:

$$\begin{aligned} \frac{P_k}{Z} &\neq n\ ;n\ is\ integer\ number \\ \frac{2P_k}{Z} &\neq n\ ;n\ is\ integer\ number \\ \frac{P_j-P_k}{Z} &\neq n\ ;n\ is\ integer\ number \\ \frac{P_j+P_k}{Z} &\neq n\ ;n\ is\ integer\ number \end{aligned} \quad (17)$$

Then, if the proposed multi-turn resolver is supposed to have P_k=1, and P_k=5, simultaneously, the undesirable number of stator teeth will be:

$$\begin{aligned} \frac{P_k}{Z} &\neq n \rightarrow Z \neq \{\varphi\} \\ \frac{2P_k}{Z} &\neq n \rightarrow Z \neq 2,10 \\ \frac{P_j-P_k}{Z} &\neq n \rightarrow Z \neq 2,4 \\ \frac{P_j+P_k}{Z} &\neq n \rightarrow Z \neq 2,6 \end{aligned} \quad (18)$$

Therefore, Z=14 is a proper choice for such resolver. The other interesting application of (17) is determining the harmonics that may interfere the main harmonic. For example, for a 5-X resolver with Z=14, some of the undesirable values for P_k are 7, 9, 14, 19, 21, 23, 28, 33, ….

Finally, the rotor shape must be designed in such a way that desirable harmonics with acceptable amplitude are involved in the teeth flux. Then, using such rotor and multiple signal windings on the stator, the proposed multi-turn resolver can be accessible.

C. Rotor Shape

The air-gap length is expressed by the Fourier series as follows:

$$g(\varphi,\theta_r) = \frac{b}{1+\sum_{k=1}^{\infty} a_k\ cos\ P_k(\varphi-\theta_r-\delta_k)} \quad (19)$$

Assigning different values for frequencies, P_k, coefficients, a_k, and the phases, δ_k, different rotor shapes are achieved. Consequently, different harmonics pass through the stator teeth. But the question that arises is "how these values should be determined to make desirable harmonics?" to answer this question, the permeance between one stator tooth and the rotor is calculated as:

$$d\rho_i = \frac{\mu_0 dA}{dg} \quad (20)$$

For sake simplicity, Cartesian coordinate system is employed and the mentioned permeance is determined by assuming parallel flux lines in the air-gap as:

$$\begin{aligned} \rho_i &= \int_x\int_z\left(\frac{1}{\int_y \frac{dg}{\mu_0 dA}}\right) = \int_x\int_z\left(\frac{\mu_0 dxdz}{g}\right) \\ &= \int_x \frac{\mu_0 L dx}{\frac{b}{1+\sum_{k=1}^{\infty} a_k\ cos\ P_k(x-x_r-\delta_k)}} \\ &= \frac{\mu_0 L}{b}\left\{x_1 + \sum_{k=1}^{\infty}\frac{2a_k}{P_k}\left(sin\left(P_k\frac{x_1}{2}-\delta_k\right)\right.\right. \\ &\left.\left.\times cos(P_k x_r)\right)\right\} = \rho_0 + \sum_{k=1}^{\infty}\rho_k\ cos(P_k x_r) \end{aligned} \quad (21)$$

where L is the stack length of the resolver and x_1 is the stator tooth width. It can be concluded from (21) that in order to achieve desirable harmonics in the teeth flux, those harmonics must be injected to the rotor contour. In Figs. 1 (a) through (d) the rotor contour for 1st, 5th, 1st and 4th, and for 1st and 5th harmonics are shown. For a multi-turn resolver consisting of both 1-speed and 5-speed sensors, the air-gap length can be determined as:

$$g(\varphi,\theta_r) = \frac{b}{1+a_1\ cos(\varphi-\theta_r)+a_5\ cos\ 5(\varphi-\theta_r)} \quad (22)$$

There are two main constraints to determine the value of b, a_1, and a_5:

1) The rotor shape's geometry must be feasible. It means the denominator of g must be positive for different values of the cosine function:

$$a_1 + a_5 < 1 \quad (23)$$

Furthermore, the rotor contour should not intersect with the rotor shaft. Therefore, the maximum air-gap length (g_{max}) must be less than $r_{si} - r_{shaft}$:

$$\frac{b}{1-(a_1+a_5)} < r_{si} - r_{shaft} \quad (24)$$

where r_{si} and r_{shaft} are the inner radius of stator and rotor shaft radius, respectively. The undesirable contours of C1 and C2, that are shown in Figs. 2 (a) and (b) respectively, present $g_{max} = r_{si} - r_{shaft}$.

This article has been accepted for publication in a future issue of this journal, but has not been fully edited. Content may change prior to final publication. Citation information: DOI 10.1109/TEC.2019.2945120, IEEE Transactions on Energy Conversion

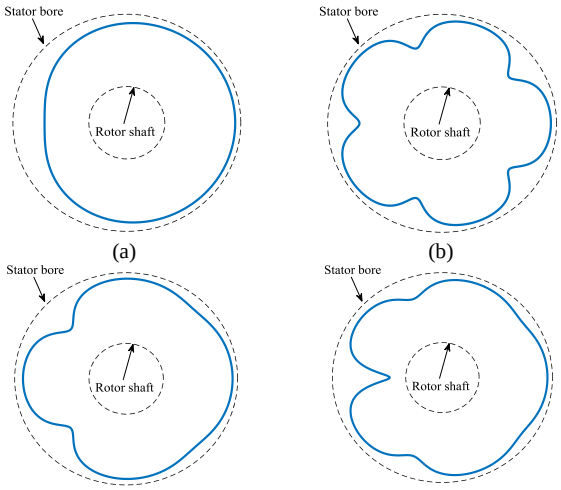

Fig. 1. Rotor Contour for different harmonic content, (a) 1st harmonic (b) 5th harmonic (c) 1st and 4th harmonic, and (d) for 1st and 5th harmonic

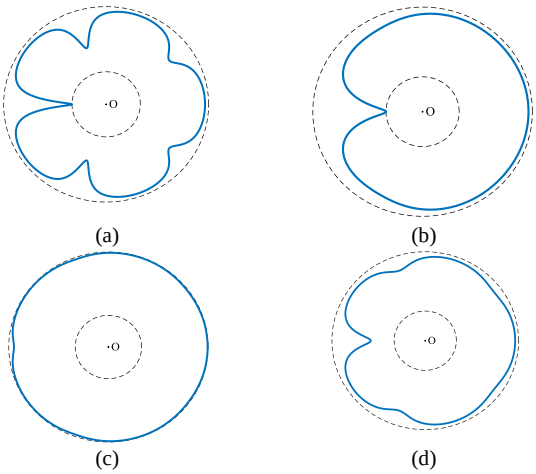

Fig. 2. Rotor Contour for different value of b, a_1, and a_5 (a) C1: b = 0.8 mm, a_1 = 0.10, and a_5 = 0.80 (b) C2: b = 0.8 mm, a_1 = 0.80, and a_5 = 0.10 (c) C3: b = 0.1 mm, a_1 = 0.36, and a_5 = 0.48 (d) C4: b = 0.8 mm, a_1 = 0.36, and a_5 = 0.48

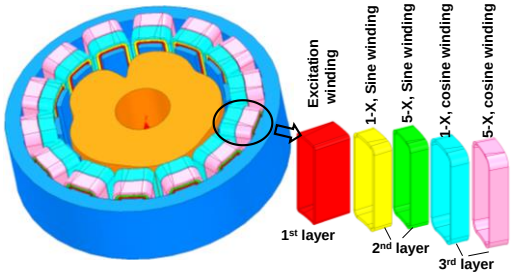

Fig. 3. The proposed multi-turn resolver

2) The maximum of air gap permeance for the desirable pole numbers must be significantly higher than that of the dc component. It means:

$$\rho_k \gg \rho_0 \, , \, a_k \, sin\left(P_k \frac{x_1}{2} - \delta_k\right) \gg P_k \frac{x_1}{2} \qquad (25)$$

Therefore, a_1 and a_5 must have large values. In Figs. 2 (a) and (b), C1 and C2 show the rotor contours for the low value of a_1 and a_5, respectively.

To choose b it should be noted that the large value of b causes infeasibility in the geometrical shape. While, the low value of b, leads to a uniform air-gap length that is undesirable, too (contour C3 in Fig.2 (c)).

Considering the mentioned constraints, the contour of C4 with b = 0.8 mm, a1 = 0.36, and a5 = 0.48, as shown in Fig. 2 (d), is used for the proposed multi-turn resolver.

In the next section, the performance of the proposed resolver is evaluated using time stepping finite element analysis.

IV. Finite Element Analysis

Time variant finite element analysis is employed to evaluate the performance of the proposed multi-turn resolver. The considerations of finite element analysis of resolvers include mesh operation, time step and stop time setting, boundary conditions, excitation method, and material assigning are taken into account [32].

Fig. 3 shows the designed resolver. It can be seen the rotor shape is determined based on (21), stator teeth number and the pole number of the consisted resolvers are determined based on (17). Two groups of signal windings are located on each stator tooth. The turn number of each signal winding is calculated using (3)– (4) after calculating the proper winding pole pairs using (2). Considering (2), P_w for 2-pole resolver is calculated equal to 6 and for 10-pole resolver, P_w=2. As mentioned earlier, the winding pole pair (P_w) for excitation winding is equal to $Z/2$. Therefore, the turn number of excitation coils can be calculate using (4). By considering the maximum turn number of the excitation and the signal coils

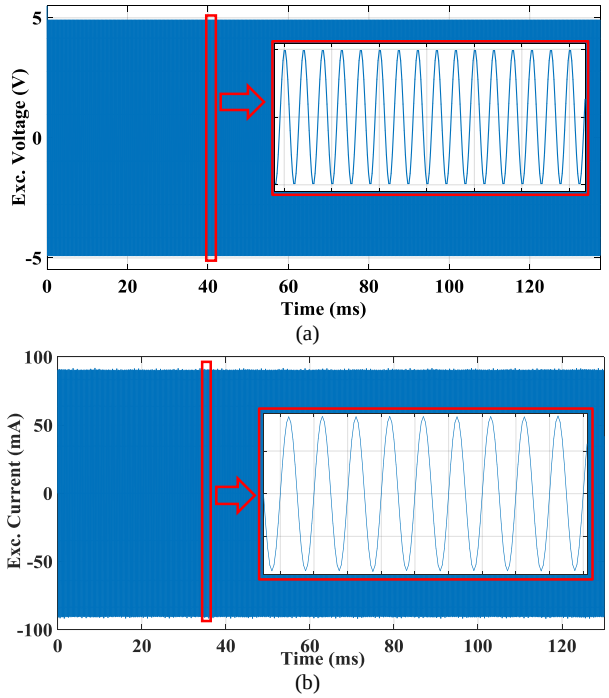

Fig. 4. The excitation of the proposed resolver: (a) the excitation voltage, and (b) the excitation current

This article has been accepted for publication in a future issue of this journal, but has not been fully edited. Content may change prior to final publication. Citation information: DOI 10.1109/TEC.2019.2945120, IEEE Transactions on Energy Conversion

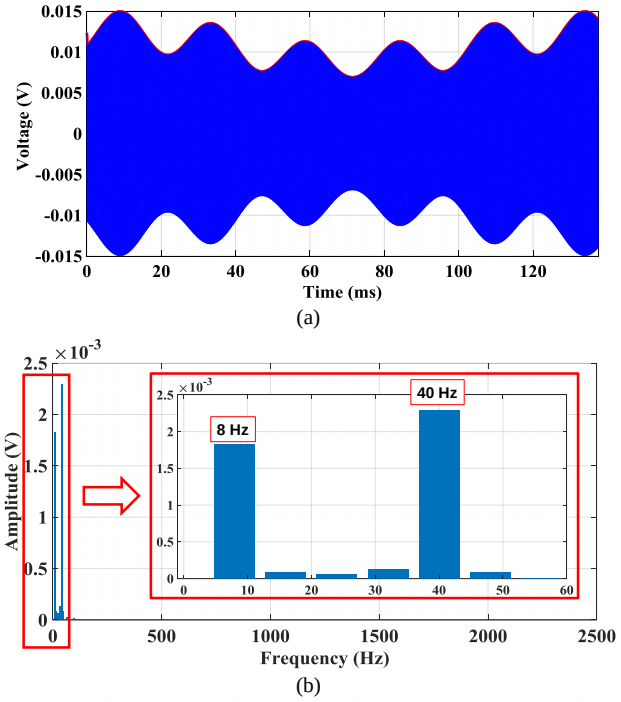

Fig. 5. The induced voltage in a coil of stator and its envelope's harmonic content: (a) the induced voltage, and (b) harmonic content of the voltage's envelope

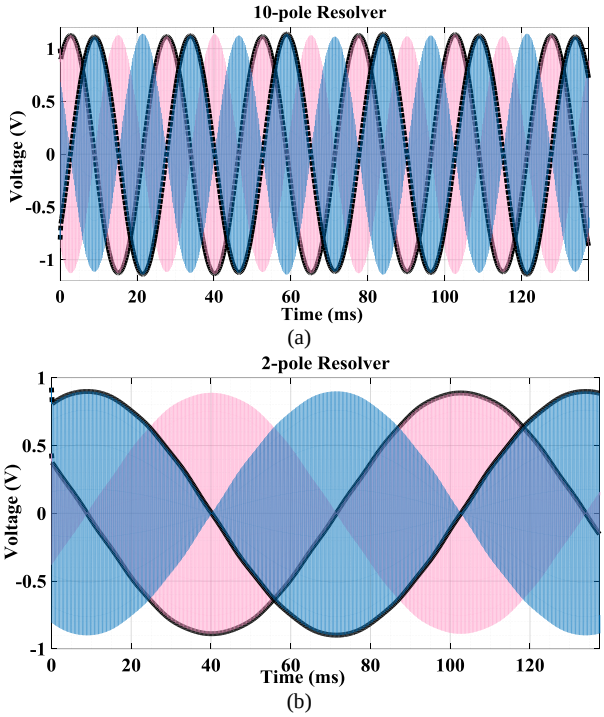

Fig. 6. The induced voltages of multi-turn resolver: (a) 10-pole resolver, and (b) 2-pole resolver

(N_{max}) equal to 30 and 70, respectively, the turn number of the excitation and signals' winding are obtained as shown in Fig. 9.

As mentioned earlier, the favorable performance of the resolver is achieved when the self-inductance of the excitation winding is constant. So, by feeding the excitation winding using a sinusoidal voltage with constant frequency and amplitude, a sinusoidal current with the same frequency will flow in the excitation winding. Fig. 4-a, and 4-b shows the excitation voltage and the excitation current of the proposed resolver. As it can be seen the amplitude of the excitation current is constant and it has the same frequency of the excitation voltage.

Furthermore, the rotor shape is determined in such a way that desirable harmonics be involved in the harmonic content of the induced voltages' envelope. The induced voltage in one stator's coil and its envelope's harmonic content are presented in Figs. 5-a, and 5-b. it can be seen in Fig. 5-b, that in addition to 40 Hz dominant harmonic which referred to 10-pole application, there is also an 8 Hz dominant harmonic that referred to 2-pole resolver.

Finally, the induced voltages in 2- and 10-pole resolver's signal windings are presented in Figs. 6-a, and 6-b, respectively. The position error of the 2-pole and 10-pole resolvers are shown in Figs. 7-a, and 7-b, respectively. It can be seen that the maximum position error (MPE) of the 1-X and 5-X resolvers is 0.72 ˚ and 0.15 ˚, respectively. The average of absolute position error (AAPE) for the single- and multi-speed resolvers is 0.24˚, and 0.07˚, respectively.

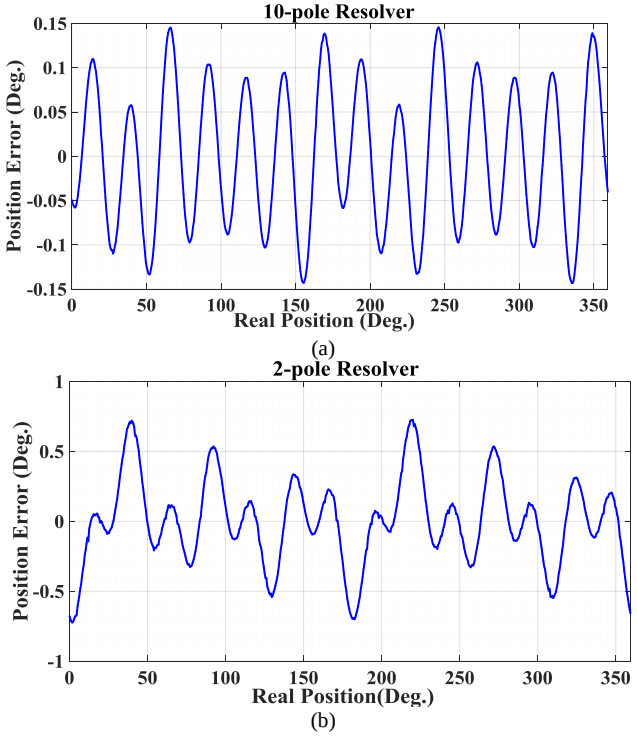

Fig.7. the position error of the multi-turn resolver: (a) 10-pole resolver and (b) 2-pole resolver

V. Experimental Tests

In order to validate the mathematical calculations and finite element analysis, a prototype of the proposed resolver is built. The geometrical characteristics of the prototype are presented in Table. I. Both the stator and the rotor cores are built using wire-cut method. The rotor and the unwound stator are shown

in Figs. 8-a, and 8-b. The schematic of stator windings is given in Fig. 9. As it can be seen from Fig. 9, the maximum number of coils on each stator tooth is five coils. The diameter of the employed copper wire is 100 µm. Fig. 10-a, shows the stator after finishing the winding process. The assembled resolver in its frame is presented in Fig. 10-b. Then, the test circuit of the prototype is given in Fig. 11. It can be seen that the prototype is coupled to a DC motor to be rotated with a constant speed. The employed motor is also coupled to an optical encoder that is used as a reference position sensor. A digitally synthesized function generator is used for feeding the excitation winding. The amplitude of the excitation voltage is adjusted to 5 V using an automatic gain control circuit and its frequency is set to 5 kHz with the resolution of 0.1 Hz. Then, the induced voltages are sampled and captured using a two-channel digital oscilloscope, as shown in Figs. 12-a, and 12-b.

Table I. Geometrical dimensions of prototype

Parameter		Unit	Value
Outer/inner diameter of stator		mm	40/24
Shaft diameter		mm	16
Maximum/ minimum air gap length		mm	5.00/0.43
	b	mm	0.80
Rotor contour parameters:	a_1		0.36
	a_5		0.48
Stack length		mm	10
Stator slot opening height/width		mm	0.60/2.00
Maximum Number of signal coil turn		-	70
Maximum Number of excitation coil turn		-	30
Number of stator teeth		-	14

(a) (b)

Fig. 8. The prototype: (a) rotor, and (b) unwound stator

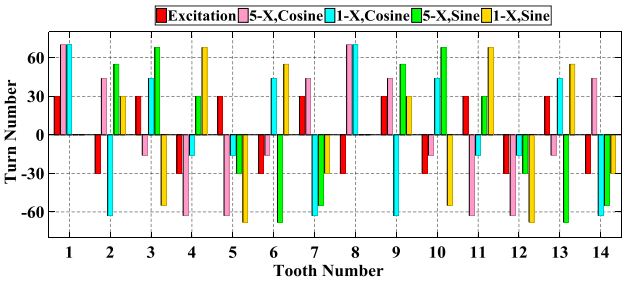

Fig. 9. The schematic of stator windings

(a) (b)

Fig. 10. The prototype multi-turn resolver: (a) the wound stator, and (b) the assembled resolver in its frame

the sampled voltages are exported to the MATLAB software and Hilbert transform is used for decoupling the high frequency excitation voltage and calculating the envelope of the signals. Afterwards, the angular position is determined by the inverse tangent of the envelopes' ratio. Comparing the calculated position with the reference position of encoder gives the position error of the single- and multi-speed sensors. The MPE and AAPE of the 1-X, and 5-X resolvers are compared with the predictions of the finite element analysis in Fig. 12-c.

The measured value of the MPE for the 1-X resolver is 0.78˚ while it has been predicted using TSFEM equal to 0.72 ˚. Considering the 5-X resolver the measured MPE is 0.16˚while it has been calculated equal to 0.15 ˚ using the TSFEA. Comparing the measured value of AAPE of the 1-X resolver (0.26˚) with the calculated values of TSFEM (0.24˚) shows the error of 8.8% between the simulation and experimental results. That compassion for the 5-X resolver (0.076˚ from measured

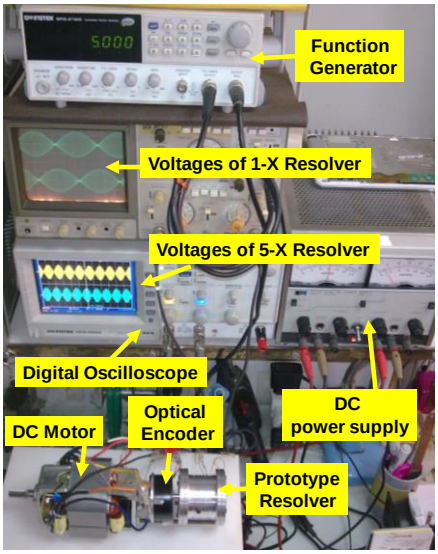

Fig. 11. The test circuit of the prototype multi-turn resolver

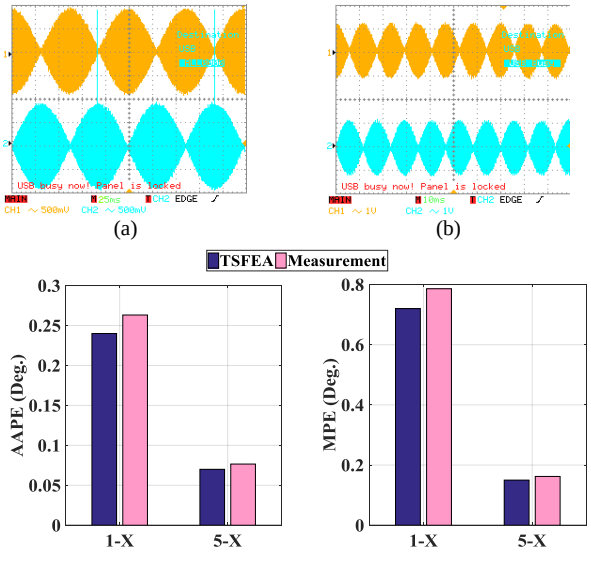

Fig. 12. the measured results: (a) the induced voltages of 1-X resolver (Time div. =25 ms, and volt div.=500mV), (b) the induced voltages of 5-X resolver (Time div. =10 ms and volt div.=1V), and (c) the position errors

signals, and 0.07 ° from TSFEM) shows 8.6% error between the measured and simulated results. Finally, it can be concluded the experimental measurements successfully validate the proposed mathematical analysis and finite element simulations.

VI. Conclusion

In this paper, a multi-turn sinusoidal air-gap length resolver was proposed. The proposed resolver had only one stator core and one rotor core and its multi-turn function was achieved by special shape of rotor contour and two-set of signal windings on the stator. Two, single speed and multi-speed, resolvers were designed in such a way that their operation have no interference with each other. Using only one core for two resolvers of presented multi-turn resolver had the advantages of saving ferromagnetic material, smaller size and lower price in comparison with conventional multi-turn resolver. The mathematical analysis of the proposed resolver has been verified by time stepping finite element analysis and experimental measurements on the prototype of the sensor.

References

[1] F. Tootoonchian, "Design and Optimization of a Multi-Turn Variable Reluctance Resolver", *IEEE Sensors Journal*, early access

[2] S. Hajmohammadi, R. Alipour-Sarabi, Z. Nasiri-Gheidari, and F. Tootoonchian, "Design Considerations of Multi-Turn Wound-Rotor Resolvers", Power Electronics, Drive Systems and Technologies Conference (PEDSTC), Shiraz, Iran, 2019.

[3] T. Miya, "Double Variable Reluctance Resolver for a Multiple Speed", United States Patent, US 7,157,906 B2, Jan. 2, 2007

[4] Position Transducers/Decoders, Handbook of Autotech Controls Company. Availabble on-line at www.avg.net

[5] J. Kessier, "Synchro/Resolver Conversion Handbook", Forth Edition, Data Device Coporation DDC.

[6] Z. Nasiri-Gheidari, "Design, Performance Analysis, and Prototyping of Linear Resolvers", *IEEE Energy Conversion*, Vol. 32, no. 4, pp. 1-10, Dec. 2017

[7] R. Alipour-Sarabi, Z. Nasiri-Gheidari, F. Tootoonchian A. Oraee, and F. Zare, "Linearized Resolver," 26th Iranian Conference on Electrical Engineering (ICEE2018), Mashhad, Iran, pp. 1191-1196, 2018.

[8] H. Saneie, Z. Nasiri-Gheidari, F. Tootoonchian, "An Analytical Model for Performance Prediction of Linear Resolver", *IET Electric Power Applications*, Vol. 11, no. 8, pp. 1457-1465, Sep. 2017

[9] A. Farhadi-Beiranvand, R. Alipour-Sarabi, Z. Nasiri-Gheidari, and F. Tootoonchian, "Selection of excitation Signal Waveform for Improved Performance of Wound Rotor Resolver", Power Electronics, Drive Systems and Technologies Conference (PEDSTC), Shiraz, Iran, 2019

[10] Z. Nasiri-Gheidari, R. Alipour-Sarabi, F. Tootoonchian and F. Zare, "Performance Analysis and Prototyping of Disk Type Variable Reluctance Resolvers", *Sensors J.*, vol. 18, no. 13, pp. 5284-5290, 2018.

[11] H. Lasjerdi, Z. Nasiri-Gheidari, F. Tootoonchian, "Proposal of an Analytical Model for Performance Evaluation of WR-Resolvers under Short Circuit Fault", 27th Iranian Conference on Electrical Engineering (ICEE2019), Yazd, Iran, 2019.

[12] F. Tootoonchian, "Effect of Damper Winding on Accuracy of Wound-Rotor Resolver under Static-, Dynamic and Mixed-Eccentricities", *IET Electric Power Applications*, vol. 12, no. 6, pp. 845-851, 7 2018.

[13] A Daniar, Z Nasiri-Gheidari, F Tootoonchian, "Position Error Calculation of Linear Resolver under Mechanical Fault Conditions", *IET Science, Measurement & Technology*, vol. 11, no. 7, pp. 948 - 954, 2017.

[14] Z. Nasiri-Gheidari, F. Tootoonchian, and F. Zare "Design Oriented Technique for Mitigating Position Error Due to Shaft Run-out in Sinusoidal-Rotor Variable Reluctance Resolvers," *IET Electr. Power Appl.*, vol. 11, no. 1, pp. 132 – 141, 2017.

[15] Z. Nasiri-Gheidari, F. Tootoonchian, "Axial flux resolver design techniques for minimizing position error due to static eccentricities", *IEEE Sensors Journal*, vol. 15, no. 7, pp. 4027-4034, July 2015

[16] F. Zare, Z. Nasiri-Gheidari, and F. Tootoonchian, "The effect of winding arrangments on measurement accuracy of sinusoidal rotor resolver under fault conditions", *Measurement*, vol. 131, pp. 162-172, 2019.

[17] F. Abolqasemi-Kharanaq, R. Alipour-Sarabi, Z. Nasiri-Gheidari, F. Tootoonchian, "Magnetic Equivalent Circuit Model for Wound Rotor Resolver without Rotary Transformer's Core", *IEEE Sensors J.*, vol. 18, no. 21, pp. 8693-8700, 1 Nov.1, 2018.

[18] H. Saneie, Z. Nasiri-Gheidari, F. Tootoonchian, "Design-Oriented Modeling of Axial-flux Variable-reluctance Resolver Based on Magnetic Equivalent Circuits and Schwarz–Christoffel Mapping", *IEEE Transactions on Industrial Electronic*, vol. 65, no. 5, pp. 4322-4330, May 2018

[19] R. Alipour-Sarabi, Z. Nasiri-Gheidari, F. Tootoonchian and H. Oraee, "Analysis of Winding Configurations and Slot-Pole Combinations in Fractional-Slots Resolvers," *IEEE Sensors J.*, vol. 17, no. 14, pp. 4420-4428, July15, 2017.

[20] R. Alipour-Sarabi, Z. Nasiri-Gheidari, F. Tootoonchian and H. Oraee, "Performance Analysis of Concentrated Wound-Rotor Resolver for Its Applications in High Pole Number Permanent Magnet Motors," *IEEE Sensors J.*, vol. PP, no. 99, pp. 1-1, 2017.

[21] R. Alipour-Sarabi, Z. Nasiri-Gheidari, F. Tootoonchian and H. Oraee, "Improved Winding Proposal for Wound Rotor Resolver Using Genetic Algorithm and Winding Function Approach," *IEEE Trans. Ind. Electron.*, vol. 66, no. 2, pp. 1325-1334, Feb. 2019.

[22] X. Ge, Z. Q. Zhu, R. Ren and J. T. Chen, "A Novel Variable Reluctance Resolver with Nonoverlapping Tooth–Coil Windings," *IEEE Trans. Energy Convers.*, vol. 30, no. 2, pp. 784-794, Jun 2015

[23] X. Ge, Z. Q. Zhu, R. Ren, J. T. Chen "A Novel variable reluctance resolver for HEV/EV applications", *IEEE Trans. Ind. Appl.*, Vol. 52, no. 4, pp. 2872 - 2880, July-Aug. 2016.

[24] K. Kim, "Analysis on the characteristics of variable reluctance resolver considering uneven magnetic fields," *IEEE Trans. Magn*., vol. 49, no. 7, pp. 3858-3861, Jul. 2013.

[25] H. Saneie, Z. Nasiri-Gheidari, F. Tootoonchian, "Accuracy Improvement in Variable Reluctance Resolvers", *IEEE Trans. Energy Convers.*, early access

[26] X. Ge and Z. Q. Zhu, "A novel design of rotor contour for variable reluctance resolver by injecting auxiliary air-gap permeance harmonics," *IEEE Trans. Energy Convers*., vol. 31, no. 1, pp. 345–353, Mar. 2016.

[27] A. Daniar, Z. Nasiri-Gheidari and F. Tootoonchian, "Performance Analysis of Linear Variable Reluctance Resolvers Based on Improved Winding Function Approach," *IEEE Trans. Energy Convers.*, vol. 33, no. 3, pp. 1422-1430, Sept. 2018.

[28] Dynapar Engineering Team, "Encoders and Resolvers: How to Choose the Right Feedback Option", www.dynapar.com

[29] Pancake Resolvers Handbook, General Dynamics Mission Systems, Availabble on-line at gdmissionsystems.com

[30] T. Miya, "Redundant resolver system", European Patent Application, EP 1 473 548 A2, 2004

[31] W. Shimizu; A. Yamashita, "Multiple Output Rotational Position Detection Device", United States Patent, US 4,604,575, 1986

[32] H. Saneie, R. Alipour-Sarabi, Z. Nasiri-Gheidari, F. Tootoonchian, "Challenges of Finite Element Analysis of Resolvers", *IEEE Trans. Energy Convers.*, early access